IJE TRANSACTIONS C: Aspects Vol. 35 No. 12, (December 2022) 2337-2343

International Journal of Engineering

Journal Homepage: www.ije.ir

Numerical Investigations of Damage Behaviour at the Weld/Base Metal Interface

S. Talouti*[a], D. Benzerga[a], H. Abdelkader[b]

[a] *LSCMI, University of Sciences and Technology of Oran, Mechanical Department, Oran, Algeria*
[b] *Univ. Artois, IMT Lille Douai, Junia, Univ. Lille, ULR 4515, Laboratoire de Génie Civil et géo Environnement (LGCgE), Béthune, France*

PAPER INFO

Paper history:
Received 03 May 2022
Received in revised form 07 July 2022
Accepted 09 September 2022

Keywords:
Welding Defect
Hydrostatic Test
Non-destructive Test
Interface
Damage
Numerical Simulation

ABSTRACT

In the present paper, the numerical modelling to predict the interface damage of weld defect in a steel pipeline was studied. This work focused on determination of the maximum operating pressure and the characterisation of mechanical behaviour at a weld-base metal interface. The operating pressure can fluctuate leading to the phenomenon of fatigue and consequently to the failure of pipeline. Experimental investigations were carried out using non-destructive test (NDT) in order to locate and determine size of defects. A bilinear interface decohesion model is used to simulate the damage behaviour considering a stress-relative displacement laws. Numerical simulations based on the finite element method were used to study the influence of size defects and young's moduli ratio on the operating pressure as well as interfacial damage between the weld and base metal. The obtained results showed that the interface damage depending on shape and material properties of defects has an impact on pipeline safety and integrity.

doi: *10.5829/ije.2022.35.12c.09*

1. INTRODUCTION

Weld defect is one of the most significant threats to onshore pipelines that can have consequences for environment due to the dangerousness of transport fluids. These macro-defects result from the micro-defects growth due to internal pressure [1-3]. Micro-defects are incorporated during the welding procedure. There are many types of welding defects that affect the performance of a product such as incomplete penetration (or lack of penetration), porosity, cluster porosity, incomplete fusion, suck back, cracks, undercut, slag, etc. Inspection of welded joints may be done using destructive methods (such as tension, shear, or bending tests) or non-destructive methods. The non-destructive testing methods that are typically used for the inspection of weldments include visual inspection, dye penetrant inspection, magnetic particles inspection, radiography and ultrasonic inspection [4]. Eshtayeh et al. [5] have shown that the digital image correlation (DIC) method can be successfully and easily used as a non-destructive inspection tool for detecting internal defects in welded joints which cannot be detected using visual inspection. The DIC method is capable of detecting the existence of different types of welding defects such as incomplete penetration, incomplete fusion, slag inclusion, cluster porosity, and such back as well as the apparent linear size of the defect.

Deivanai and Soni [6] concluded that the NDT can be applied on all type of materials including composite materials and allowed to identify surface subsurface and internal defects ensuring quality of materials and joining processes without destroying them. The effect of defect on toughness behaviour of pipeline steels is studied by Vijay Kumar Dalla [7] using facture and failure analysis. The authors showed that fracture toughness is reduced by 68 % due to influence of microstructure. Pipeline failure also depends on cycling loading due to the operating pressure of the fluids and corrosion [8-10]. Many methods have addressed accessing fatigue life performance, like empirical model using a safe-life approach, fracture mechanics method, and statistical based on probability models [11-13]. Damage by pitting corrosion of the surface areas of the local oil and gas pipelines was identified and numerically analysed by Maruschak et al. [14, 15]. They concluded that the

* Corresponding author Email: *said.talouti@yahoo.com* (S. Talouti)

Please cite this article as: S. Talouti, D. Benzerga, H. Abdelkader, Numerical Investigations of Damage Behaviour at the Weld/Base Metal Interface, ***International Journal of Engineering, Transactions C: Aspects***, Vol. 35, No. 12, (2022), 2337-2343

decrease of the structural strength of oil and gas pipelines is due to reduction of the cross section, caused by corrosion; softening because of stress relaxation; formation of defects, such as micro cracks; and fragility influenced by hydrogen action. Also, they demonstrated that increase in fatigue crack length is accompanied by the increase in the size of plastic deformation zone near the crack tip that makes the transition from the quasi-brittle failure to the fatigue one with the formation of fatigue striations. It is known that crack initiation and propagation can be occurred at the weld defect and base metal interface. Debonding of the interface is one of an undesirable failure mechanism. This paper presents the analysis of numerical modelling based on the indirect use of fracture mechanics to determine the behaviour of weld defect – pipeline interface. The model is based on NDT method to detect metallurgical defects that could represent a potential source of damage. Both approaches, NDT and numerical, offer an alternative to the destructive methods such as hydrostatic test to predict the interface damage that causes failure of pipeline.

Our study focuses on the interface damage of a weld defect which is supposed to have a spherical shape, embedded in a matrix of a micro-alloyed steel gas pipeline. The interface model assumes a bilinear softening behaviour of the interfacial provided with stress-relative displacement laws. This work is carried out using the finite element code (ANSYS*)* in association with a house program to simulate decohesion at the interface (inclusion/matrix) and its effect on the macroscopic behaviour of the structure.

2. NUMERICAL MODELING

Gas pipelines are obtained by welding operations from sheets. The molten pool created during welding operation is characterized by a very complex thermophysical processes involving thermal, convective, chemical and electromagnetic phenomena depending on the nature of the process used [11]. These convection movements of the liquid or gaseous metal significantly influence the shape of the weld bead and the heat transfers can induce defects such as inclusions or porosities. These defects are generally too small to be detectable by the non-destructive method, called NDT [12]. Generally, failure results from the germination, growth and coalescence of defects at the microscopic scale. These cavities originate from inclusion/matrix decohesion [13, 15]. The model used for the numerical simulations is composed of an incompressible matrix and a cavity possibly filled by a spherical inclusion. The matrix represents the representative elementary volume of a pipe in which the defect is embedded. This matrix is supposed to be elastoplastic, whereas the material which constitutes the inclusion can be purely elastic in the case of rigid defects or elastoplastic in the case of ductile defects. The inclusion that represents the defect is initially assumed to be perfectly spherical [16]. The matrix behaviour subjected to an internal pressure is studied under a pure tension loading [17, 18]. Due to the symmetry, only a quarter of body is modelled. The following boundary conditions were chosen: constraints on one side of the matrix – inclusion and an applied displacement on the other side, as shown in Figures 1 and 2.

Taking into account the symmetry of the structure, we mesh only a quarter of model. The structure has been discretized using a four-node quadrilateral element mesh for both matrix and inclusion, as shown in Figure 3. The inclusion is assumed to have a spherical shape embedded in a matrix of X65 pipeline steel. The displacement was imposed in the tangential direction due to the value of the tangential stress (hoop stress) which is equal to the double of the axial and radial stress ($\sigma_{\text{hoop}} = 2\sigma_{\text{axial}} = 2\sigma_{\text{radial}}$).

The main inclusions present in X65 steel of this study are the tungsten and copper inclusions coming from the TIG and MIG welding process, respectively [19, 20].

The proposed interfacial damage model is considered as a two dimensional entity, taking into account two decohesion modes which ensure traction stress σ_n and shear stress t_n [21, 22]:

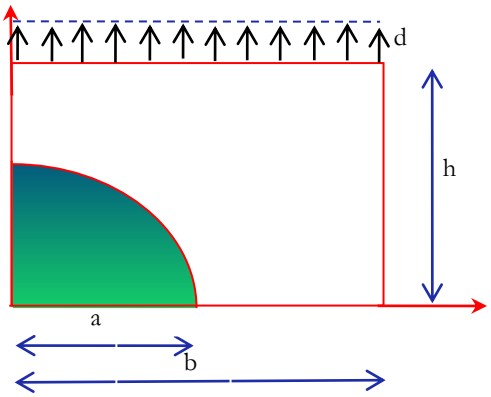

Figure 1. Weld defect as an inclusion and matrix model

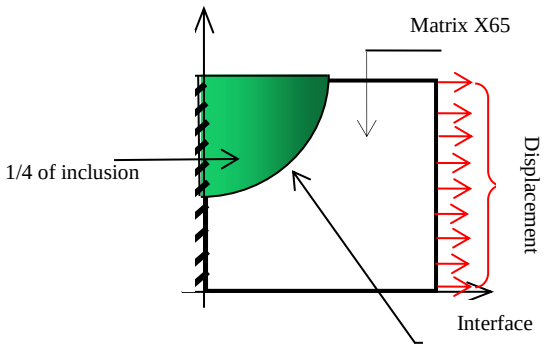

Figure 2. Applied boundary conditions

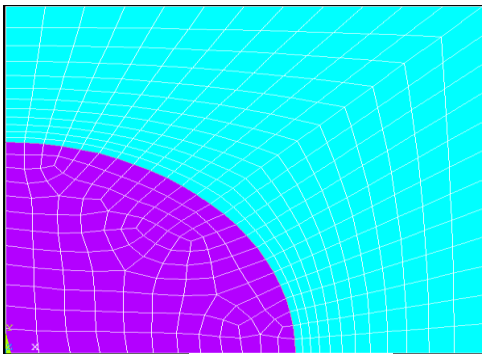

Figure 3. Finite element model

$$\left(\frac{\sigma_n}{\hat{\sigma}_n}\right)^2+\left(\frac{t_n}{\hat{t}_n}\right)^2=1 \quad \text{for} \quad \sigma_n>0 \tag{1}$$

$\hat{\sigma}_n$ et $\hat{t}_n$ are the ultimate traction and shear strengths of the interface, respectively. By introducing an evolution law of the ultimate stress $\hat{\sigma}_n$

$$\begin{gathered}(\sigma_n)^2+\left(\frac{\hat{\sigma}_n}{\hat{t}_n}\right)^2(t_n)^2=(\hat{\sigma}_n)^2 \Rightarrow \\ \begin{bmatrix}\sigma_n & t_n\end{bmatrix}\begin{bmatrix}1 & 0\\ 0 & \left(\frac{\hat{\sigma}_n}{\hat{t}_n}\right)^2\end{bmatrix}\begin{bmatrix}\sigma_n\\ t_n\end{bmatrix}=(\hat{\sigma}_n)^2\end{gathered} \tag{2}$$

The interface behaviour can be described by a bilinear relationship between the traction and relative displacement (see Figure 4)

The interface model (Equation (1)) is reconsidered as a plasticity criterion with softening:

$$\sqrt{\sigma^T A\sigma}-\hat{\sigma}_n(u)=f(\sigma)-\hat{\sigma}_n(u)=0 \text{ for } \sigma_n>0 \tag{3}$$

with

$$\begin{gathered}u=\langle\delta-\delta_0\rangle \\ \langle x\rangle=\begin{cases}x \text{ if } x\geq 0\\ 0 \text{ if } x<0\end{cases}\end{gathered} \tag{4}$$

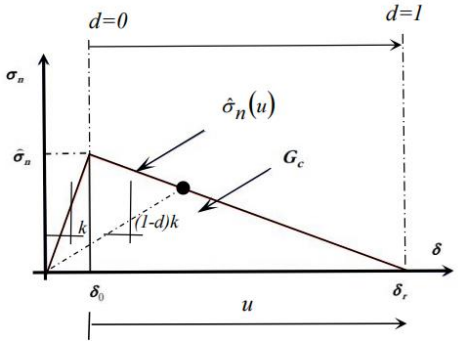

Figure 4. Bilinear interface decohesion model

δ represents the relative interfacial displacement.

Considering a bilinear behaviour of the interface [23] See Figure 4, the term $\hat{\sigma}_n(u)$ can be expressed as follows:

$$\hat{\sigma}_n(u)=\hat{\sigma}_n(1-\omega u) \quad \text{with} \quad \omega>0 \tag{5}$$

The parameter ω is derived from critical energy G_C that represents the surface under the curve (Figure 4) [24]:

$$\omega=\frac{\hat{\sigma}_n e}{2G_C} \tag{6}$$

e denotes the thickness of the interface.

The relationship (3) shows that when $f(\sigma)$ reaches the threshold $\hat{\sigma}_n$ ($\delta=\delta_0$ corresponds to $u=0$ and u will be calculated from the relationship 5). At this moment, we have an initiation of the decohesion at the interface. The decohesion is complete when $\hat{\sigma}_n(u)$ reaches a zero value for interfacial displacement ($\delta=\delta_r$) threshold of total decohesion and opened surfaces are completely free of stresses.

To develop an interface model damage, it is assumed that the mechanical behaviour of the interface $(\hat{\sigma}_n-\delta)$ follows the law described in Figure 4, where $\delta=\delta_0$ et $\delta=\delta_r$ correspond to the displacements obtained for the maximum stress $\hat{\sigma}_n$ and at the final rupture of the interface when the stress vanishes. A damage variable can be expressed as follows [25-27]:

$$d=\begin{cases}0 \Leftarrow \delta\leq\delta_0\\ \dfrac{\hat{\sigma}_n-\hat{\sigma}_n(u)}{\hat{\sigma}_n} \Leftarrow \delta_0<\delta<\delta_r\\ 1 \Leftarrow \delta>\delta_r\end{cases} \tag{7}$$

Taking into account the damage, the behaviour of the interface is given by the following relations:

$$\begin{Bmatrix}\sigma_n\\ \tau_n\end{Bmatrix}=\begin{bmatrix}(1-d)k_n & 0\\ 0 & (1-d)k_t\end{bmatrix}\begin{Bmatrix}\delta_n\\ \delta_t\end{Bmatrix} \tag{8}$$

where k_n and k_t are the stiffnesses of the interface in the normal and tangential direction. d_n and d_t are the interfacial relative displacements (see Figure 4). To illustrate the progression of interfacial decohesion, when $d= 1$ describes total decohesion which means that the absolute value of the interlaminar stress vector is reduced to zero.

3. APPLICATION OF THE METHOD

Recent developments in digital image processing and computer vision have enabled the introduction of a new automated vision system for the detection and evaluation of gas pipeline weld defects from radiographic films. This new system makes it possible to detect welding

defects and estimate the necessary information such as the length, width, area, orientation, angle and perimeter of the defects. It offers many advantages such as eliminating the need for image interpretation by specialist inspectors and the ability to enhance captured images so that defects appear much clearer (see Figure 5) [28].

Among the welding defects, taken within the framework of this study, the inclusions of tungsten and copper resulting from the processes of welding TIG and MIG respectively. Tungsten particles embedded in welds (Generally GTAW only) are very hard and can cause very intense local residual stresses. These defects come from too small tungsten electrodes, too high and amperage, AC balance on +, Upslope too high, electrode tip not snipped, electrode dipped into the weld pool or touched with the fill rod, electrode split**.** These tungsten inclusions are detected by x-ray and show up as bright particles since they are much denser than the steel (see Figure 6).

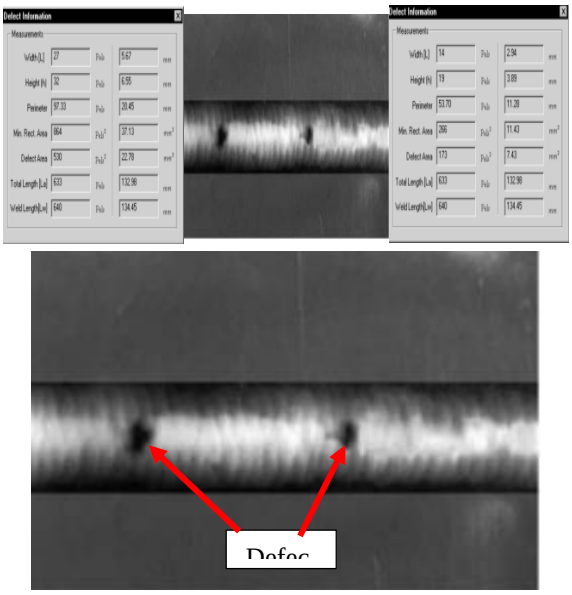

Figure 5. Captured radiographic image [24]

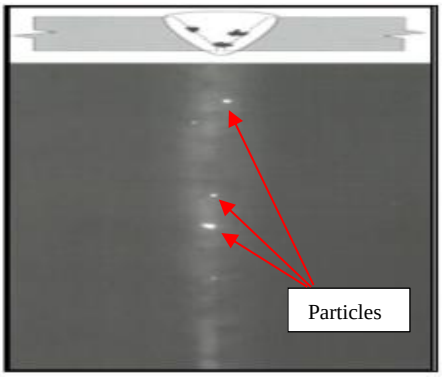

Figure 6. Tungsten inclusions

It can also happen that copper inclusions enter the weld pool. This is the case when copper welding consumables come into contact with the weld pool, or when the copper gas nozzle comes into contact with the weld pool or the seam preparation side. Copper inclusions are extremely difficult to detect with non-destructive testing. These inclusions cause embrittlement of the weld. The previously developed decohesion model has been translated into APDL language and implemented in the ANSYS finite element code. The interface was modelled using the CZM interface element [29]. Interface surfaces are represented by a special set of interface elements or contact elements. In the case of CZM, decohesion is treated as a progressive phenomenon in which cohesive tensile separation takes place across a cohesive zone. The extension of this cohesive zone in front of the crack tip is modelled using the tensile separation laws (also called the cohesion law) which links the cohesive stress to the separation in the process zone. First, we studied the effect of Young's modulus of the inclusion on the macroscopic behaviour of the structure. In a second step, the effect of inclusion size was considered to highlight this parameter on the global behaviour of the structure. The defects are embedded in a matrix of API 5L X65 pipeline steel [30] (see Table 1).

To highlight the effect of mechanical resistance of the inclusion on the macroscopic behaviour, we have examined several ratios: Young's modulus of the inclusion / Young's modulus of the matrix (E_{in}/E_{mat}).
In the case of a ratio (E_{inc}/E_{mat}=0.7), Figure 7(a) shows that the deformation of matrix and inclusion is homogeneous and the decohesion is small compared with the ratio E_{inc}/E_{mat} =3.5 in Figure 7(b). In this Figure 7(b), the decohesion is important at the tops of the inclusion; this is due to the rigidity of the tungsten inclusion; the deformation is inhomogeneous. This shows that the decohesion is more important for a hard inclusion (E_{inc}/E_{mat} =3.5) than a ductile inclusion (E_{inc}/E_{mat}=0.7). This behaviour leads to anisotropic damage at the interface.

Figure 8 shows the effect of inclusions of different resistances on the macroscopic behaviour. We clearly see the effect of Young's moduli of the defect, i.e. of the inclusion, on the macroscopic level. When the inclusion is hard with a high elastic modulus, the initiation of its interfacial damage occurs for lower stress levels compared to softer inclusions (Figure 8). It should be noted, after initiation of damage (critical zone), that the curves representing the hard inclusions are characterized by a strain hardening more important than the ductile

TABLE 1. API 5L X65 mechanical properties

Young's modulus	Poisson's ratio	Yield strength	Tensile strength
210 (GPa)	0.3	450 (MPa)	535 (MPa)

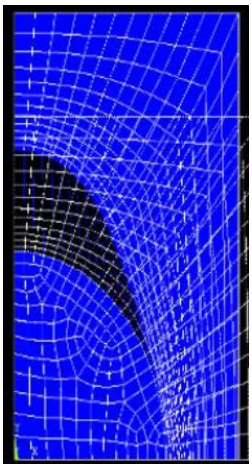

(a) Inclusion of tungsten

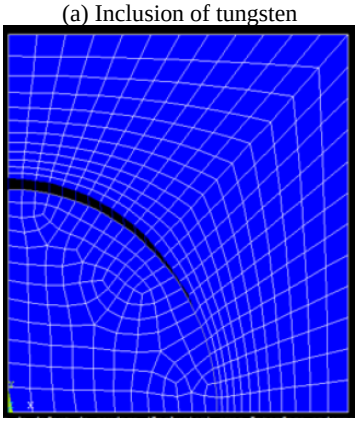

(b) Inclusion of copper

Figure 7. Damage behaviour at matrix-inclusion interface

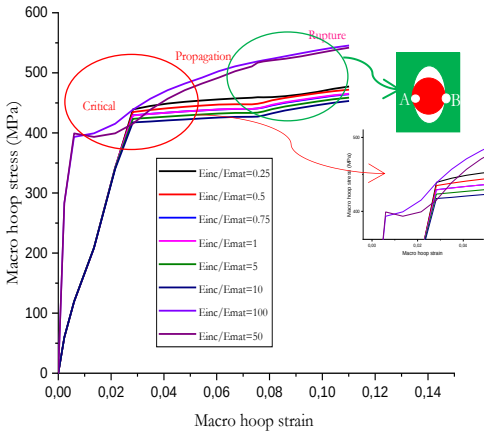

Figure 8. Effect of inclusion strength on macroscopic behaviour

inclusions. This can be explained by the great resistance that a hard inclusion opposes to zones A and B when it is subjected to the compression caused by the matrix during external static loading. This behaviour leads to anisotropic damage at the interface. The effect of dynamic loading on changes in the mechanical properties and crack resistance of the pipe steel has been studied by Chausov et al. [31].

Figure 9 shows the effect of defect strength (Young's modulus of inclusion) on interfacial damage pressure. It can be noted, from Figure 7, the decohesion is higher for hard inclusions ($E_{incl}/E_{mat} > 2$) causing failure of structure if hydrostatic test is performed. From a ratio E_{incl}/E_{mat} higher than 5, defects cannot withstand fluctuations of operating pressure as function of time. The defect of tungsten with a ratio equal to 3.5 (TIG welding) cannot withstand the hydrostatic test.

The propagation can cause the variation of the operating pressure. While in the case of copper defect (MIG welding) with a ratio equal to 0.7, the structure can withstand to the hydrostatic test.

Figure 10 highlights the influence of defect size on the interfacial damage between the inclusion and the X65 matrix. This figure shows the behaviour of copper and

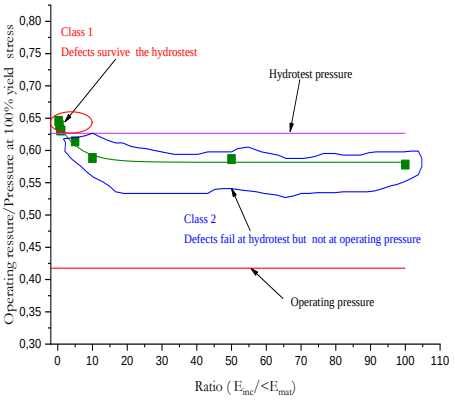

Figure 9. Interfacial damage pressure values for inclusion of radius 5µm

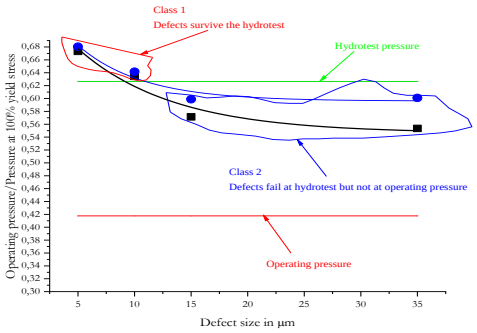

Figure 10. Interfacial damage pressures for tungsten and copper defects

tungsten defects for different sizes. It is observed that at small size defect, the operating pressure is high due to the toughness of inclusion, but at greater size defect, the operating pressure is small because of the ductility of inclusion. In conclusion, we can say that the damage of matrix – inclusion interface occurs rapidly for a hard inclusion than for a ductile inclusion.

4. CONCLUSION

In the present work, numerical simulation associated with NDT method has shown that it could replace destructive methods such as hydrostatic test to predict the failure of pipeline. Numerical results using interface model have been presented to predict the damage process at a matrix weld defect interface. This damage model was based on the indirect use of fracture mechanics considering a softening stress-relative displacements law. Different size defects and young's moduli ratios were used and a numerical predicted was developed to separate the failure and safe zones for damage of matrix - weld defect interface. For lower young's moduli and size defect ratios, no failure of structure was observed if hydrostatic test is performed. An excessive rise young's moduli and size defect ratios has not an impact on the rupture of structure. Not only the elastoplastic properties of the affected material (degradation of elastic moduli, decrease in elastic limit, etc.), but there is also a significant softening effect on the macroscopic behavior as well as anisotropy. The results obtained show that the rigid interfaces fail rapidly, while the soft interfaces, in spite of a weakening effect of the material, have a slow fail.
This approach, numerical modelling associated with NDT method, will certainly be more economic than hydrostatic test.

5. REFERENCES

1. Adjogbe, S., Okoronkwo, C., Oguoma, O., Igbokwe, J. and Okwu, M., "Investigation of the effect of hydrostatic pressure testing on the microstructure of carbon steel pipeline material", ***AASCIT Journal of Materials***, Vol. 4, No. 3, (2018), 58-65.
2. Matta, L., "Collective effects of leakage, temperature changes, and entrapped air during hydrostatic testing", in Pipeline Pigging and Integrity Management Conference., (2017).
3. Bulatovic, S., Aleksic, V. and Milovic, L., "Failure of steam line causes determined by ndt testing in power and heating plants", ***Frattura ed Integrità Strutturale***, Vol. 7, No. 26, (2013), 41-48. doi: 10.3221/IGF-ESIS.26.05.
4. Khan, M.I., "Welding science and technology, New Age International, (2007).
5. Eshtayeh, M., Hijazi, A. and Hrairi, M., "Nondestructive evaluation of welded joints using digital image correlation", ***Journal of Nondestructive Evaluation***, Vol. 34, No. 4, (2015), 1-12. doi: 10.1007/s10921-015-0310-z.
6. Deivanai, S. and Soni, M., "Non destructive testing and analysis of friction stir welded aluminium alloy 2024 pipes", ***Materials Today: Proceedings***, Vol. 56, (2022), 3721-3726. https://doi.org/10.1016/j.matpr.2021.12.470
7. Dalla, V.K., "Experimental investigation of fracture behavior and microstructure of api 5lx60 line pipe", ***Materials Today: Proceedings***, Vol. 56, (2022), 595-608. https://doi.org/10.1016/j.matpr.2021.12.149
8. Adjogbe, A., Okoronkwo, C., Igbokwe, J., Ezurike, O. and Oguoma, O., "The impact of hydrostatic pressure test on the interstitial strength of mild-steel pipeline material", ***Indian Journal of Science and Technology***, Vol. 12, (2019), 43. doi: 10.17485/ijst/2019/v12i43/144730.
9. Balamuralikrishnan, R., Krishnamurthy, B. and AlHarthy, M.N., "Destructive and non-destructive testing methods for condition monitoring of concrete elements", ***Journal of Multidisciplinary Engineering Science and Technology***, Vol. 4, No. 6, (2017).
10. Foorginejad, A., Taheri, M. and Mollayi, N., "A non-destructive ultrasonic testing approach for measurement and modelling of tensile strength in rubbers", ***International Journal of Engineering, Transactions C: Aspects,*** Vol. 33, No. 12, (2020), 2549-2555. doi: 10.5829/ije.2020.33.12c.16.
11. Bilat, A.-S., "Estimation du risque de rupture fragile de soudures de pipelines en aciers à haut grade: Caractérisation et modélisation", Paris, ENMP, (2007),
12. Allouti, M., "Etude de la nocivité de défauts dans les canalisations de transport de gaz tels les éraflures, les enfoncements ou leurs combinaisons", Université Paul Verlaine-Metz, (2010),
13. Ramière, I., Masson, R., Michel, B. and Bernaud, S., "Un schéma de calcul multi-échelles de type éléments finis au carré pour la simulation de combustibles nucléaires hétérogènes", in 13e colloque national en calcul des structures., (2017).
14. Maruschak, P., Prentkovskis, O. and Bishchak, R., "Defectiveness of external and internal surfaces of the main oil and gas pipelines after long-term operation", ***Journal of Civil Engineering and Management***, Vol. 22, No. 2, (2016), 279-286. doi: 10.3846/13923730.2015.110067.
15. Maruschak, P., Panin, S., Stachowicz, F., Danyliuk, I., Vlasov, I. and Bishchak, R., "Structural levels of fatigue failure and damage estimation in 17mn1si steel on the basis of a multilevel approach of physical mesomechanics", ***Acta Mechanica***, Vol. 227, No. 1, (2016), 151-157. https://doi.org/10.1007/s00707-015-1420-5
16. Czarnota, C., "Endommagement ductile des matériaux métalliques sous chargement dynamique-application à l'écaillage", Université de Metz, (2006),
17. Regad, A., Benzerga, D., Berrekia, H., Haddi, A. and Chekhar, N., "Repair and rehabilitation of corroded hdpe100 pipe using a new hybrid composite", ***Frattura ed Integrità Strutturale***, Vol. 15, No. 56, (2021), 115-122. doi: 10.3221/IGF-ESIS.56.09
18. Berrekia, H., Benzerga, D. and Haddi, A., "Behavior and damage of a pipe in the presence of a corrosion defect depth of 10% of its thickness and highlighting the weaknesses of the asme/b31g method", ***Frattura ed Integrità Strutturale***, Vol. 13, No. 49, (2019), 643-654. doi: 10.3221/IGF-ESIS.49.58
19. Gupta, M., Shukla, S.K., Sharma, V.K. and Kumar, H., "Effect of tig and mig welding on microstructural and mechanical properties: Astate of art", ***International Journal of Applied Engineering Research***, Vol. 13, No. 9, (2018), 83-90.
20. Chaht, F.L., Mokhtari, M. and Benzaama, H., "Using a hashin criteria to predict the damage of composite notched plate under traction and torsion behavior", ***Frattura ed Integrità Strutturale***, Vol. 13, No. 50, (2019), 331-341. doi: 10.3221/IGF-ESIS.50.28.
21. Benzerga, D., Haddi, A., Seddak, A. and Lavie, A., "A mixed-mode damage model for delamination growth applied to a new

woven composite", ***Computational materials science***, Vol. 41, No. 4, (2008), 515-521. doi: 10.1016/j.commatsci.2007.05.022.

22. Orangi, R., Mansourian, H., Bina, K. and Rabbanifar, S., "Vulnerability assessment of steel structures in district 12 of mashhad city and prioritizing the welding defects using the analytic hierarchy process", ***International Journal of Engineering***, Vol. 31, No. 6, (2018), 877-885. doi: 10.5829/ije.2018.31.06c.03.
23. Li, S., Zhang, L., Sun, Q. and Tengfei, M., "Numerical simulation method study of rock fracture based on strain energy density theory", ***Frattura ed Integrità Strutturale***, Vol. 13, No. 47, (2019), 1-16. doi: 10.3221/IGF-ESIS.47.01.
24. Wagner, W. and Gruttmann, F., "Delamination growth analysis of composite panels", ***Revue Européenne des Eléments***, Vol. 13, No. 8, (2004), 915-929. doi: 10.3166/reef.13.915-929.
25. Wu, Q. and Wang, Y., "Experimental detection of composite delamination damage based on ultrasonic infrared thermography", ***International Journal of Engineering, Transactions B: Applications*** Vol. 27, No. 11, (2014), 1723-1730. doi: 10.5829/idosi.ije.2014.27.11b.10.
26. Sprenger, W., Gruttmann, F. and Wagner, W., "Delamination growth analysis in laminated structures with continuum-based 3d-shell elements and a viscoplastic softening model", ***Computer Methods in Applied Mechanics and Engineering***, Vol. 185, No. 2-4, (2000), 123-139. doi: 10.1016/S0045-7825(99)00255-8.
27. Saboori, B. and Moshrefzadeh-sani, H., "A continuum model for stone-wales defected carbon nanotubes", ***International Journal of Engineering***, Vol. 28, No. 3, (2015), 433-439. doi: 10.5829/idosi.ije.2015.28.03c.13.
28. Gobbi, G., Colombo, C. and Vergani, L., "A cohesive zone model to simulate the hydrogen embrittlement effect on a high-strength steel", ***Frattura ed Integrità Strutturale***, Vol. 10, No. 35, (2016), 260-270. doi: 10.3221/IGF-ESIS.35.30.
29. Shafeek, H., Gadelmawla, E., Abdel-Shafy, A. and Elewa, I., "Assessment of welding defects for gas pipeline radiographs using computer vision", ***NDT & e International***, Vol. 37, No. 4, (2004), 291-299. doi: 10.1016/j.ndteint.2003.10.003.
30. Benzerga, D., "Burst pressure estimation of corroded pipeline using damage mechanics", in Conference on Multiphysics Modelling and Simulation for Systems Design, Springer., (2014), 481-488.
31. Chausov, M., Maruschak, P., Pylypenko, A. and Sorochak, A., Effect of impact-oscillatory loading on the variation of mechanical properties and crack resistance of pipe steel, in Degradation assessment and failure prevention of pipeline systems. 2021, Springer.189-201.

Persian Abstract

چکیده

تست های هیدرواستاتیک پس از تحقق تاسیسات مشمول مقررات از جمله: سازه های متمرکز، لوله ها، لوله کشی، تجهیزات استاتیک، مخازن تحت فشار، مخازن و غیره از اهمیت بالایی برخوردار است. بازرسی جوش ها اغلب با آزمایش هیدرواستاتیک با فشار ۱.۵ برابر فشار سرویس تضمین می شود و در حضور ضروری نماینده ARH (مرجع تنظیم کننده هیدروکربن ها) انجام می شود. تجهیزات تحت فشار تحت بازرسی NDT (تست غیر مخرب) برای تأیید اجرای صحیح جوش ها و آزمایش هیدرواستاتیک برای تأیید یکپارچگی آنها قرار می گیرند. تکنسین ها با محدودیت های زیادی در جداسازی تجهیزات مواجه می شوند تا آن ها را در اختیار بخش تست هیدرواستاتیک قرار دهند. بنابراین کاملاً واضح است که آزمایشات هیدرواستاتیکی یک ناراحتی واقعی برای مدیریت سازه های جوش داده شده است. هدف از این کار نشان دادن این است که تکنیک‌های بازرسی NDT با شبیه‌سازی‌های عددی می‌توانند یک راه‌حل جایگزین برای جایگزینی آزمایش‌های هیدرواستاتیکی باشند. برنامه ای در APDL در کد Ansys برای شبیه سازی وابستگی رابط (شامل/ماتریس) و تأثیر آن بر رفتار ماکروسکوپی سازه توسعه یافته و پیاده سازی شده است.